33rd Annual International Conference of the IEEE EMBS
Boston, Massachusetts USA, August 30 - September 3, 2011

Automated patient couch removal algorithm on CT images

Peter Bandi, Norbert Zsoter, Laszlo Seres, Zoltan Toth, Laszlo Papp

Abstract— **The current paper proposes a novel automated patient couch removal method on Computed Tomography (CT) images. Patient couch is often considered to be an unnecessary artifact especially when 3D rendered techniques are used. The method is based on measuring similarity between selected axial slices and the assumption that the bed object is constant on different slices. Due to the weight of the patient the couch could bend which is identifiable as sagittal movement on consecutive axial slices. Therefore the method focuses on finding this movement after an initial segmentation. According to initial validation performed on real medical data, our method is an effective tool to remove patient couch without user interaction.**

I. INTRODUCTION

Computed tomography (CT) is one of the most widely used morphological modalities in radiology and nuclear medicine [1], [3]. The CT visualization is done with both 2D and 3D rendering techniques depending on the type of the daily routine [5], [8], [9]. Due to the CT imaging technology patient couch is always present on reconstructed images. Since the patient couch does not hold useful information for evaluation, it is an unnecessary artifact on medical viewers. Furthermore, due to the nature of some rendering techniques like 3D Volume Rendering (VR) [2], [4] and Maximum Intensity Projection (MIP) [5], [6] the patient couch is even disturbing when it hides important anatomical information (see Fig. 4). Therefore an automated patient couch removal is required.

The segmentation of the patient couch is a challenging task, since the patient may touch the couch hence simple threshold methods cannot separate them (see Fig. 1) [6]. Furthermore the couch may move along the axial slices due to non-uniform distribution of the patient's weight over it [3], [9] (see Fig. 2).

Considering the difficulties mentioned above, our goal was to propose an automated method which copes with both patient couch movements and couch - patient connections. We built on the idea of detecting slightly changing objects over the axial slices and we assumed that body regions change faster than the shape of the couch.

II. MATERIALS AND METHODS

A. Patient images

Forty reconstructed anonymized human whole body CT images were collected in Digital Imaging and Communication in Medicine (DICOM) format acquired by 4 different camera vendors (10 for all vendors). All 3D reconstructed images consisted an ordered series of 2D axial slices having equal pixel resolution (in our case 512×512).

P. Bandi, N. Zsoter, L. Seres and L. Papp are with Mediso Medical Imaging Systems Ltd., Baross str. 91-95, Budapest, Hungary peter.bandi@mediso.hu

Zoltan Toth is with Scanomed Ltd., Budapest, Hungary zoltan.toth@ymail.com

B. Methods

We assumed that the shape of the couch was very similar over axial slices, but little movements could occur (see Fig. 2) and patient could even touch the couch (see Fig. 1).

The method had five main steps: feature extraction, initial couch localization, couch movement detection, couch mask generation and couch removal.

1) Feature extraction: The method built on the high similarly of couch shape over the axial slices, therefore lower body similarities had to be assured. Since body regions were also very similar between neighboring slices, the feature extraction step had to decrease the body region similarity compared to the similarity of the couch. This was achieved by not processing all slices but only a subset of them as follows:

Let us denote I as the input CT with k slices, furthermore $S_j \in I$ as the j^{th} axial slice of I where $0 \leq j < k$. Let us denote $M_p \subseteq I$ a subset containing S_i slices chosen from I with normal distribution as defined by (1).

$$M_p = \left\{ S_0, S_q, S_{2q}, \ldots, S_{\lfloor \frac{k-1}{q} \rfloor q} \right\} \tag{1}$$

where $q = \left\lfloor \frac{1}{p} \right\rfloor$. Therefore every q^{th} slice was collected to M_p. Based on initial trials $p = 0.1$ was an appropriate choice.

Let us denote $(x, y) \in \mathbb{N}^2$ a pixel coordinate inside of $S_i \in M_p$ where $S_i(x, y)$ represents the value at the x^{th} row and y^{th} column in S_i. Multiple low-high cut was performed on all $S_i \in M_p$ slices defined as (2).

$$\forall (x, y) : S_i^c(x, y) = min\left(max\left(Lc, S_i(x, y)\right), Hc\right) \tag{2}$$

where $Lc = -400$ and $Hc = 400$ are low and high cut values according to standard Hounsfield Scale [10]. The Lc and Hc threshold values were determined by initial trials. The multiple cut was necessary to remove artifacts (inlays, implants, background noise, etc.) from the CT that could mislead our method. The result of the cut was collected to M_p^c where $M_p^c = \{S_i^c | S_i \in M_p\}$.

Multiple correlation was performed among all $S_i^c \in M_p^c$ slices to create a two dimensional C correlation slice where $C(x, y)$ was defined by (3).

$$C(x,y) = \sum_{a=-n}^{n} \sum_{b=-n}^{n} \prod_{S_i^c \in M_p^c} (S_i^c(x+a, y+b) - m_i(x,y)) \tag{3}$$

where $\forall (x,y), \forall i \mid S_i^c \in M_p^c : m_i(x,y)$ was defined as (4).

$$m_i(x,y) = \sum_{a=-n}^{n} \sum_{b=-n}^{n} \left(\frac{S_i^c(x+a, y+b)}{(2n+1)^2} \right) \tag{4}$$

where the correlation disk size was $2n+1$ which determined a $(2n+1)^2$ sized pixel area. According to initial trials $n = 4$ was chosen.

2) Initial couch localization: A binary thresh was applied on C correlation slice to generate a B binary mask slice as defined by (5).

$$\forall (x,y) : B(x,y) = \begin{cases} 0 & \text{if} \quad C(x,y) = 0 \\ 1 & \text{otherwise} \end{cases} \tag{5}$$

Although the feature extraction step decreased the similarity of body regions, artifacts remained on the binary image. In order to remove these artifacts, the disjunct regions (having value 1) of B were labeled in B^r with unique values (see Fig. 3). Then the w_s weight of each s region was calculated by summing the distances of each pixel of the region from the center of the slice to identify the heaviest one as defined by (6).

$$w_s = \sum_{B^r(x,y)=s} d(x,y)^e \tag{6}$$

where $d(x,y)$ is the distance of (x,y) from the geometric center of the slice. According to initial trials $e = 4$ was an appropriate choice. The label value with the heaviest weight was chosen. All other values in B^r were changed to 0.

The B^r image was an initial mask, in which misclassification of the values was possible. In order to decrease the possibility of patient couch border exclusion, a morphologically dilated B^d slice was generated from B^r [7] as defined by (7) (see Fig. 3).

$$B^d(x,y) = \max_{\substack{x-n \le i \le x+n \\ y-n \le j \le y+n}} (B^r(i,j)) \tag{7}$$

The number of positive values in image B^d was counted and stored in $b \in \mathbb{N}$ value.

3) Couch movement detection: Current step determined the relative shifting value $\delta_i = (k,l)$ $(\delta_i \in \mathbb{Z}^2)$ between $S_{i-1}^c \in M_p^c$ and $S_i^c \in M_p^c$ which gave the best fit of these slices as defined by (8).

$$\delta_i = \arg\min_{a,b} \sum_{x,y} \frac{\left(S_{i-1}^c(x,y) - S_i^c(x+a, y+b)\right)^2}{b} \tag{8}$$

where $B^d(x,y) > 0$, $-\phi \le a,b \le \phi$ and $a,b \in \mathbb{Z}$. The ϕ value represented the maximal expected shift in each direction. Based on initial trials $\phi = 2$ was an appropriate choice. Note that $\delta_0 = (0,0)$ as the first slice was the reference slice.

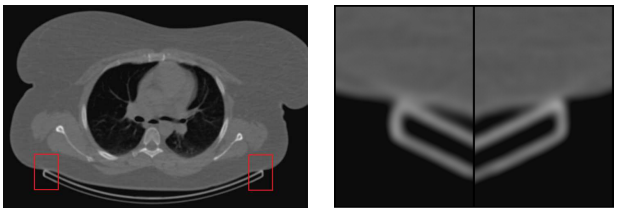

Fig. 1. An axial CT slice where the patient couch is connected with the patient (left). The magnified regions of the red rectangles (right).

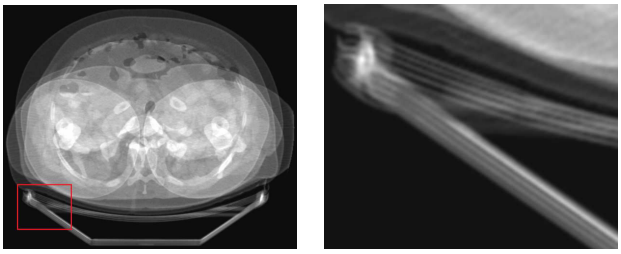

Fig. 2. Six averaged axial slices representing body and couch changes over the axial slices. (left). The magnified view of the red rectangle represents slight patient couch movements (right).

4) Couch mask generation: According to the determined δ_i which represented a relative shifting between $S_i^c \in M_p^c$ and $S_{i-1}^c \in M_p^c$ consecutive slices, $\epsilon_i \in \mathbb{Z}^2$ was defined representing the shifting relative to the first S_0^c slice by (9).

$$\forall i | S_i^c \in M_p^c : \epsilon_i = \sum_{j=0}^{i} \delta i \tag{9}$$

Using the shifting values of ϵ_i, S_i^t slices were generated from applying the ϵ_i translation on the corresponding $S_i^c \in M_p^c$ slice.

By having the translated S_i^t slices were the corresponding couch regions were overlapping, a final D mask slice was generated by applying multiple correlation on S_i^t images as defined by (3).

The D slice was then threshed as shown in (5).

Since the D mask slice could have represented a hollow patient couch mask, it was filled in by vertical sweeping lines (see Fig. 3).

5) Couch removal: Based on the D mask slice, $\Delta_j \in \mathbb{Z}^2$ shifting values were determined for all $S_j \in I$ slices. For all j^{th} slices the enclosing $i = \left\lfloor \frac{j}{q} \right\rfloor$ and $i+q$ sample slice indices were determined to identify ϵ_i and ϵ_{i+q}. The final shifting coordinates of Δ_j were linearly interpolated by the values in ϵ_i and $\epsilon i + q$ as defined by (10).

$$\Delta_j = \frac{(i+q-j)\epsilon_i + (j-i)\epsilon_{i+q}}{q} \tag{10}$$

A D_j mask slice was created for all $S_j \in I$ slices by shifting D mask with corresponding Δ_j. The final I' image was created by (11).

(B) (B^d) (D)

Fig. 3. The initial B mask slice representing labeled regions (left), the filtered and dilated B^D slice mask (middle) and the filled D slice mask (right)

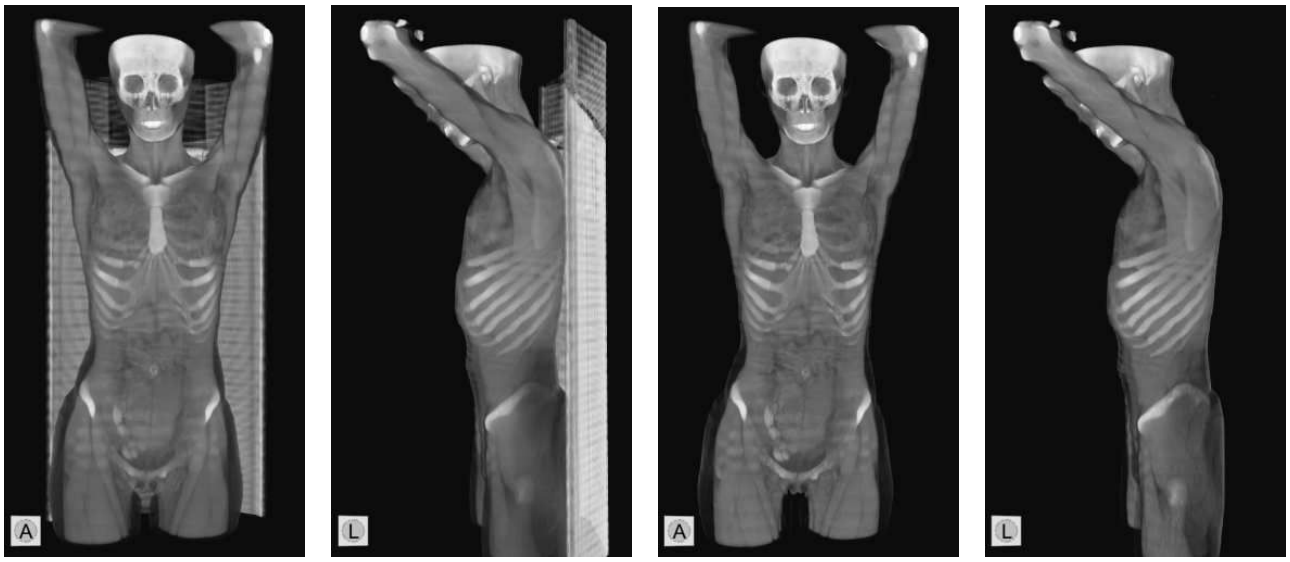

Fig. 4. Different volume rendering views of a female patient before and after the couch removal method.

$$\forall\ 0 < j \leq k : S'_j(x,y) = \begin{cases} \min(I) & \text{if} \quad D_j(x,y) > 0 \\ S_j(x,y) & \text{otherwise} \end{cases} \tag{11}$$

where $S'_j \in I'$ is the j^{th} slice in image I' and $\min(I)$ denoted the minimum value of the original I image.

C. Validation

Validation was performed by radiologists who evaluated our method in all individual cases. There were three possible outcomes of an evaluation: passed (couch was successfully removed), failed (couch was not removed) partially passed (the couch was not removed completely). The validation was done by investigating the axial as well as the volume rendering views of the given CT representing the before - after stage.

III. RESULTS

Based on the validation performed on the collected images, our method successfully removed 95% of the patient couches, while 5% was partially removed. In the problematic cases, however, increasing the n and p walues led to an acceptable result. The scoring statistics for all camera vendors is detailed in Tab. I. Overall average $<$ 1sec processing time was necessary to run our method on a typical whole body CT image (approx. 300 slices).

TABLE I

EVALUATION STATISTICS OF OUR METHOD

Camera vendor	Passed	Partially passed	Failed
Vendor 1	9	1	0
Vendor 2	10	0	0
Vendor 3	9	1	0
Vendor 4	10	0	0

IV. CONCLUSIONS AND FUTURE WORKS

A. Conclusions

We presented an accurate and quick patient couch removal method which did not need any user interaction. Our method did not provide acceptable result in some cases due to the empiric p and n parameters, but modifying these values always led to acceptable results. This means that changing n and p variables automatically based on properties derived from the input image, a more accurate result could be achieved.

B. Future Works

We will collect more CT images from more camera vendors to accurately work out that mechanism which estimates the optimal n and p parameters of our method.

REFERENCES

[1] E. C. Beckmann, CT scanning the early days, *British Journal of Radiology*, vol. 79, 2006, pp 5-8.

[2] P. S. Calhoun, B. S. Kuszyk, D. G. Heath and et al., Three-dimensional Volume Rendering of Spiral CT Data: Theory and Method, *Radio-Graphics*, 1999, vol. 19, 745-764.

[3] W. E. Brant, C. A. Helms Fundamentals of diagnostic radiology, *in Third SIAM Conference on Applied Linear Algebra*, 3rd. ed. 2007

[4] Z. Li and J. Zhang , Study on volume rendering of CT slices based on ray casting, *in 2010 3rd IEEE International Conference on Computer Science and Information Technology (ICCSIT)*, vol. 7, 2010, pp 157.

[5] W. O. Thean, H. Ibrahim, K. Toh, Implementation of several rendering and volume rotation methods for volume rendering of 3D medical dataset, *in CITISIA 2008. IEEE Conference on Innovative Technologies in Intelligent Systems and Industrial Applications, 2008.*, 2008, pp. 49.

[6] E. Neri, D. Caramella, and C. Bartolozzi, Image Processing in Radiology: Current Applications, Medical Radiology, Springer Verlag, Berlin, Heidelberg, 2008.

[7] M. R. Haralick, R. S. Sternberg and X. Zhuang, Image Analysis Using Mathematical Morphology, *IEEE Transactions on Pattern Analysis and Machine Intelligence*, 1987, pp 532-550

[8] E. G. A. Aird and J. Conway, CT simulation for radiotherapy treatment planning, *British Journal of Radiology*, vol. 75, 2002, pp. 937-949.

[9] L. W. Goldmann, Principles of CT and CT Technology, *Journal of Nuclear Medicine Technology*, vol. 35, 2007, pp. 115-128.

[10] E. C. Beckmann, Godfrey Newbold Hounsfield, *Physics Today*, vol. 58, pp. 8485.